Polymer Bulletin (2022) 79:3333–3352
https://doi.org/10.1007/s00289-021-03675-0

ORIGINAL PAPER

Synthesis of novel aromatic polyamides containing both sulfone linkages and cardo groups by a recyclable palladium-catalyzed carbonylation and condensation polymerization

Jianying Li[1,2] · Bin Huang[1] · Huali Tang[1] · Mingzhong Cai[1]

Received: 17 November 2020 / Revised: 22 February 2021 / Accepted: 18 March 2021 /
Published online: 25 March 2021

Abstract

A series of novel aromatic polyamides containing both sulfone linkages and cardo groups were synthesized via a heterogeneous palladium-catalyzed carbonylation and condensation reaction of aromatic diiodides bearing ether sulfone linkages, carbon monoxide, and aromatic diamines with cardo groups. Polycondensation reaction proceeded smoothly under 1 atm of CO at 120 °C in *N,N*-dimethylacetamide (DMAc) by using a bidentate phosphine ligand-modified magnetic nanoparticles-anchored palladium complex [2P-Fe_3O_4@SiO_2-$PdCl_2$] as a recyclable catalyst with 1,8-diazabicycle[5,4,0]-7-undecene (DBU) as a base, furnishing cardo poly(ether sulfone amide)s with inherent viscosities between 0.70 and 0.77 dL/g. The resulting polyamides could be readily dissolved in polar aprotic organic solvents and even dissolved in less polar pyridine and tetrahydrofuran at room temperature and could be easily converted into flexible, transparent, and tough films via casting from their solutions in DMAc. These polymers exhibited excellent thermal stability with the glass transition temperatures between 241 and 283 °C and the temperatures at 5% weight loss ranging from 438 to 475 °C in an atmosphere of nitrogen. The polyamide films displayed good mechanical behavior with tensile strengths of 78.8–84.4 MPa, tensile moduli of 2.08–2.57 GPa, and elongations at breakage of 10.2–12.5%, and optically high transparency with cut-off wavelengths in the range of 338–368 nm.

Keywords Aromatic poly(ether sulfone amide) · Cardo structure · Carbonylation · Polycondensation · Heterogeneous catalysis

✉ Mingzhong Cai
caimzhong@163.com

[1] Key Laboratory of Functional Small Organic Molecule, Ministry of Education and College of Chemistry and Chemical Engineering, Jiangxi Normal University, Nanchang 330022, China

[2] School of Biology and Environmental Engineering, Jingdezhen University, Jingdezhen 333000, China

Introduction

Aromatic polyamides, such as poly(*p*-phenyleneterephthalamide) (PPTA) and poly(*m*-phenyleneisophthalamide) (MPIA), exhibit many desirable characteristics including excellent mechanical properties, high thermal stability, and good chemical resistance, along with low flammability [1–9]. Despite the outstanding combined properties, most of aromatic polyamides suffer from some drawbacks such as infusibility and limited solubility in most organic solvents because of the strong interchain interaction caused by the highly rigid and regular polymer backbone and the existence of intermolecular hydrogen bonding, which result in their poor processability and restrict their wide-spread applications. Thus, considerable efforts have been devoted to the design of the chemical structure of the rigid polymer backbone to obtain aromatic polyamides that are easily processable by traditional techniques [10–14].

On the other hand, aromatic poly(ether sulfone)s, such as those derived from 4,4′-dichlorodiphenyl sulfone and bisphenols like 2,2-bis(4-hydroxyphenyl)propane, biphenyl-4,4′-diol, and 4,4′-dihydroxydiphenyl sulfone, have already been developed into commercial high-performance thermoplastic materials because of their good mechanical properties, high thermooxidative stability, as well as excellent hydrolytic stability [15–17]. These polymers are generally amorphous and transparent materials having comparatively high glass transition temperatures and have been extensively employed as thermoplastic matrices in fiber-reinforced composites using Kevlar, carbon, and glass fibers as reinforcement [18]. It is well known that the introduction of sulfone linkages into polymer main chain could lead to an enhanced solubility, an increased T_g value, and excellent thermooxidative stability. In order to modify the properties of aromatic polyamides, aromatic poly(ether sulfone amide) s have been synthesized by low temperature solution polycondensation reactions of 4,4′-(4,4′-sulfonylbis(4,1-phenylene)bis(oxy))dianiline with diaroyl chlorides [19], 4,4′-(4,4′-sulfonylbis(4,1-phenylene)bis(oxy))dibenzoyl chloride with aromatic diamines [20], and aromatic diamines containing sulfone and amide units with diaroyl chlorides [21]. The resulting polyamides were characterized by outstanding thermooxidative stability and solubility, good mechanical behavior, and higher glass transition temperatures.

The carbonylation and condensation reactions of aromatic dihalides, carbon monoxide, and aromatic diamines under the catalysis of palladium have been developed into an alternative approach for the synthesis of aromatic polyamides due to some attractive advantages such as the elimination of corrosive and moisture-sensitive aromatic diacid chlorides, the use of CO as a inexpensive and easily available C1 source, and the easy availability of various bishalogenated arene monomers [22–30]. However, all the carbonylative polymerizations were carried out using homogeneous $PdCl_2(PPh_3)_2$ (typically 6 mol%) as the catalyst and an excess of PPh_3 as the ligand. Homogeneous catalysis suffers from the difficult separation of the palladium catalyst from the desired product and the inability to recycle the expensive catalyst. Moreover, the polycondensation catalyzed by a homogeneous palladium complex might result in a high level of residual palladium in the desired polymer because of

palladium leaching. The process for removal of palladium impurity from the resulting polymer is rather tedious since the residual palladium species was firmly embedded in the curled polymer chain, thereby limiting application of this methodology in large-scale preparation of highly purified polymers. Therefore, development of highly active and recyclable heterogeneous palladium catalysts for the carbonylative polycondensation without palladium leaching remains a challenging task and is highly desirable.

In recent years, the application of magnetic nanoparticles-bound palladium complexes in organic transformations has received much attention since the palladium complexes anchored onto magnetic nanoparticles can be facilely separated from the product and recovered simply by placing a magnet near the reaction vessel without centrifugation and/or filtration, which minimizes loss of the palladium catalyst and greatly improves its recyclability [31–35]. Recently, we have described the preparation of a bidentate phosphine ligand-modified magnetic nanoparticles-anchored palladium complex [2P-Fe_3O_4@SiO_2-$PdCl_2$] and its application to heterogeneous carbonylation and condensation reaction of aromatic diiodides, carbon monoxide, and aromatic diamines towards new aromatic polyamides [36–38]. To further expand the application of this heterogeneous palladium catalyst and examine the combined effects of sulfone linkages and cardo groups on the properties of aromatic polyamides, herein we report the synthesis of new aromatic polyamides containing both sulfone linkages and cardo groups through a heterogeneous carbonylation and condensation reaction of aromatic diiodides bearing ether sulfone linkages, carbon monoxide, and aromatic diamines with cardo groups by using 2P-Fe_3O_4@SiO_2-$PdCl_2$ as a recyclable palladium catalyst. The new polyamides obtained were characterized by FT-IR, ^{1}H-NMR, WAXD, DSC, TGA, UV–vis, etc. Primary characterization results indicated that they might serve as new candidates for solution processable high-performance engineering plastic and optoelectronic materials.

Experimental

Materials

The 2P-Fe_3O_4@SiO_2-$PdCl_2$ complex was prepared via our previously described route [36]. *N,N*-Dimethylacetamide (DMAc), *N,N*-dimethylformamide (DMF), *N*-methyl-2- pyrrolidone(NMP), 1,3-dimethyl-2-imidazolidone (DMI), dimethyl sulfoxide (DMSO), and hexamethylphosphoramide (HMPA) were purified by distillation under a reduced pressure and stored over 4 Å molecular sieve. Diphenylphosphine, 3-aminopropyltriethoxysilane, and 1,8-diazabicyclo[5,4,0]-7-undecene (DBU) were purified by distillation under a reduced pressure. 4,4′-Di(3-iodophenoxy)diphenyl sulfone (**1a**) [38], 4,4′-di(4-iodophenylsulfonyl)diphenyl ether (**1b**) [38], 9,9-bis[4-(4-aminophenoxy)phenyl]fluorene (**2a**) [39], 9,9-bis[4-(4-amino-2-trifluoromethylphenoxy)phenyl]fluorene (**2b**) [40], 9,9-bis-[4-(4-aminophenoxy) phenyl]xanthene (**2c**) [41], and 9,9-bis[4-(4-amino-2-trifluoromethylphenoxy)phenyl]xanthene (**2d**) [42] were prepared by referring to literature methods. All other

starting materials were of analytical grade and were employed as received from different commercial sources.

Characterization

FT-IR spectra of the polymers in KBr pellets were obtained with a Horiba FT-720 FTIR spectrometer. ^{1}H NMR (400 MHz) spectra were recorded on a Bruker Avance 400 (400 MHz) spectrometer in DMSO-d_6 as solvent with Me_4Si as the internal reference. Elemental analyses were conducted on a PerkinElmer model 2400 CHN element analyzer. Inherent viscosities ($\eta_{inh} = (\ln \eta_r)/c$) were measured on a Cannon–Fenske viscometer at a concentration of 0.5 g/dL in DMAc at 30 °C, in which the polyamides were pretreated by drying in oven at 120 °C for 2 h to remove the adsorbed moisture. Molecular weights were measured on a gel permeation chromatograph (GPC) with polystyrene calibration using JASCO HPLC equipped with Shodex KD-80 M column at 40 °C in DMF. Differential scanning calorimetry (DSC) analyses were conducted on a Mettler Toledo DSC 821e instrument under nitrogen protection at a heating rate of 10 °C/min, and the T_g values were read at the middle of the transition in the heat capacity in the second scan. The samples were pre-heated at 150 °C for 1 h before DSC measurements. Thermogravimetric analysis (TGA) was carried out with a Netzsch Sta 449c thermal analyzer system under nitrogen protection at a heating rate of 20 °C/min. The measurements were taken after an initial 250 °C/10 min drying step. The stress–strain behavior of the polyamide films were studied on an Instron model 1130 universal tester with 60 × 5 mm specimens at a drawing rate of 5 mm/min, and an average of at least five individual determinations was reported. Wide angle X-ray diffraction (WAXD) patterns were recorded at room temperature on a Rigaku D/MAX-IIA X-ray diffractometer with nickel-filtered CuKα radiation (40 kV and 20 mA). Ultraviolet–visible spectra of the polyamide films were obtained on a V-550 UV–vis spectrophotometer. The refractive indices of the polymer films were determined by a prism-coupler method on Sairon SPA-3000 model at 623.8 nm. The palladium content of the catalyst was measured with a Jarrell-Ash 1100 ICP analysis.

Preparation of the 2P-Fe_3O_4@SiO_2-$PdCl_2$ catalyst

A mixture of 3-(*N,N*-di(diphenylphosphinomethyl))aminopropyltriethoxysilane (0.928 g, 1.5 mmol) and Fe_3O_4@SiO_2 (1.103 g) in dry toluene (50 mL) was stirred at reflux for two days under nitrogen. After the mixture was cooled to room temperature, the resulting product was magnetically separated, followed by washing with toluene to remove the unanchored phosphine ligand and dried at 120 °C in vacuo for 4 h to afford 1.322 g of the bidentate phosphine ligand-modified Fe_3O_4@SiO_2 (2P-Fe_3O_4@SiO_2). The phosphorus content of 2P-Fe_3O_4@SiO_2 was found to be 0.96 mmol/g based on elemental analysis.

A mixture of palladium chloride (73 mg, 0.4 mmol) and 2P-Fe_3O_4@SiO_2 (1.02 g) in dry acetone (50 mL) was stirred at reflux for 3 days under N_2. After the reaction mixture was cooled to room temperature, the resulting product was magnetically

separated, followed by washing with acetone repeatedly and dried at 80 °C in vacuo for 5 h to afford 1.037 g of 2P-Fe_3O_4@SiO_2-$PdCl_2$. The palladium content of 2P-Fe_3O_4@SiO_2-$PdCl_2$ was found to be 0.38 mmol/g based on ICP-AES.

Synthesis of polymers

A 100 mL, oven-dried reaction tube equipped with a CO inlet and a magnetic stirrer was charged with 4,4′-di(3-iodophenoxy)diphenyl sulfone **1a** (0.3273 g, 0.5 mmol), DBU (0.184 g, 1.2 mmol), 2P-Fe_3O_4@SiO_2-$PdCl_2$ (79.5 mg, 0.03 mmol), 9,9-bis[4-(4-aminophenoxy)phenyl]fluorene **2a** (0.2715 g, 0.51 mmol), and DMAc (2.5 mL) under an atmosphere of nitrogen. After being evacuated, the reaction tube was back-filled with CO and sealed. The reaction mixture was then heated to 120 °C over 20 min and was stirred for 12 h at 120 °C. After being cooled to room temperature, the resulting viscous polymer solution was further diluted with DMAc (13 mL), and the catalyst was magnetically separated. The polymer solution was then trickled into MeOH (100 mL) with stirring to produce a precipitate. The white fiber-like precipitate was collected by filtration, washed with hot MeOH (3 × 20 mL) and water (2 × 20 mL) and dried at 150 °C in vacuo for 5 h to yield polymer **3aa**. The recovered palladium catalyst was washed with DMAc (2 mL), deionized H_2O (2 mL), acetone (2 mL), dried at 100 °C in vacuo for 2 h and employed directly in the next polymerization cycle. Other polymers **3ab–3bd** were also synthesized by a similar procedure as described for polymer **3aa**.

Results and discussion

Preparation of the 2P-Fe_3O_4@SiO_2-$PdCl_2$ catalyst

The bidentate phosphine ligand-modified magnetic nanoparticles-anchored palladium complex[2P-Fe_3O_4@SiO_2-$PdCl_2$] was prepared by referring to our previously reported route as illustrated in Scheme 1 [36]. The silica-coated Fe_3O_4

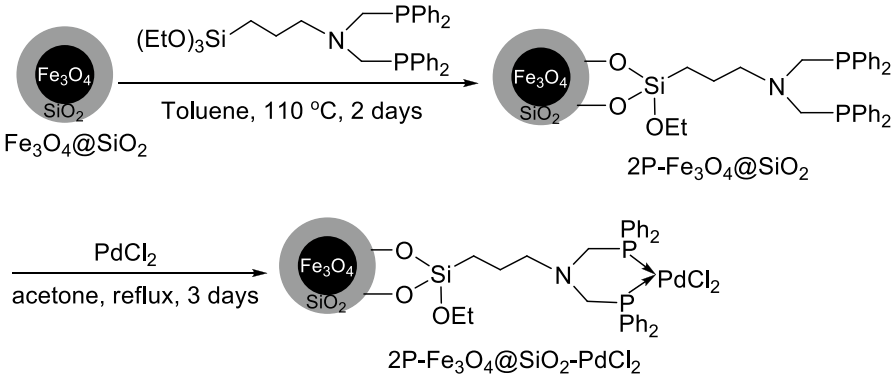

Scheme 1 Preparation of the 2P-Fe_3O_4@SiO_2-$PdCl_2$ complex

(Fe_3O_4@SiO_2) was reacted with 3-(*N*,*N*-di(diphenylphosphinomethyl))aminopropyltriethoxysilane at 110 °C in toluene under nitrogen for 2 days to give the bidentate phosphine ligand-modified magnetic nanoparticles (2P-Fe_3O_4@SiO_2). The 2P-Fe_3O_4@SiO_2 was then complexed with palladium chloride in dry acetone at reflux under nitrogen for 3 days to afford the 2P-Fe_3O_4@SiO_2-$PdCl_2$ complex. The palladium content of 2P-Fe_3O_4@SiO_2-$PdCl_2$ was found to be 0.38 mmol/g by using ICP-AES analysis.

Preparation of aromatic diiodide monomers

The synthetic routes to aromatic diiodides having ether sulfone linkages **1a** and **1b** are shown in Scheme 2 [38]. 4,4′-Di(3-iodophenoxy)diphenyl sulfone (**1a**) was obtained through the nucleophilic substitution reaction of 3-iodophenol with 4,4′-dichlorodiphenyl sulfone in toluene and DMAc with K_2CO_3 as base (Scheme 2a). On the other hand, 4,4′-di(4-iodophenylsulfonyl)diphenyl ether (**1b**) was prepared by the Friedel–Crafts acylation reaction of iodobenzene with 4,4′-oxydiphenyldisulfonyl chloride in nitrobenzene in the presence of $FeCl_3$ (Scheme 2b). The ^{1}H-NMR spectra shown in Fig. 1 were in good accordance with the proposed structures of monomers **1a** and **1b**.

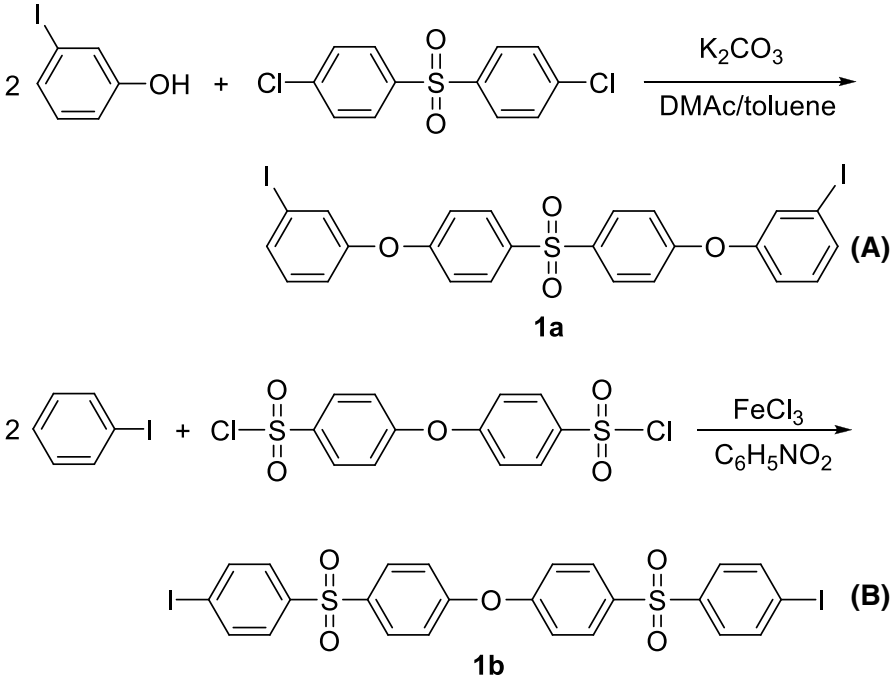

Scheme 2 Preparation of aromatic diiodide monomers **1a** and **1b**

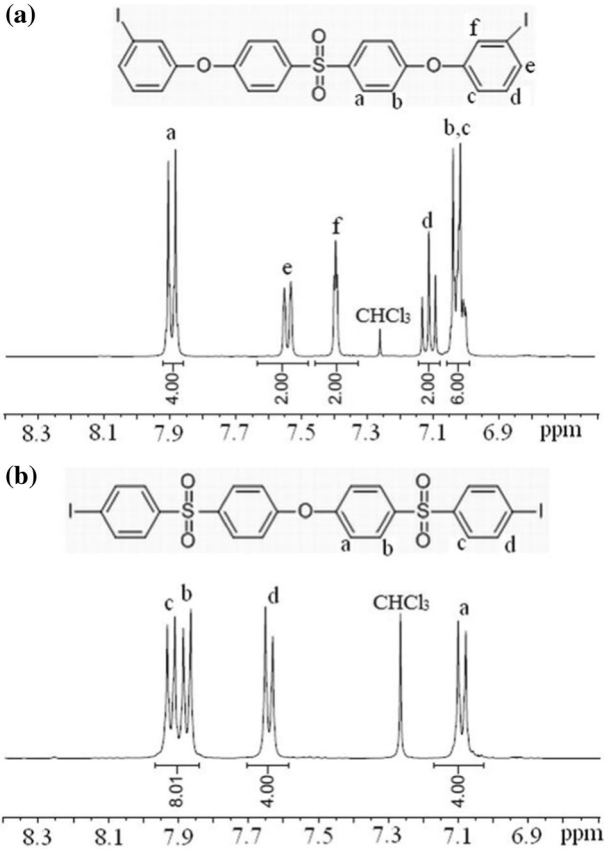

Fig. 1 ^{1}H-NMR spectra of the monomers **1a** and **1b** ($CDCl_3$)

Synthesis and characterization of polymers

Over the past decades, significant efforts have been made to design and synthesize wholly aromatic polyamides containing cardo structures. Generally, the incorporation of cardo structures into the main chains of polyamide imparts good solubility and processability, and better mechanical and thermal behaviors [39–45]. However, to our knowledge, relatively little attention has been paid to the synthesis of cardo poly(ether sulfone amide)s. To further examine the combined effects of sulfone linkages and cardo groups on the properties of aromatic polyamides, a series of novel aromatic polyamides containing both sulfone linkages and cardo groups were synthesized through a carbonylation and condensation reaction of aromatic diiodides bearing ether sulfone linkages, carbon monoxide, and aromatic diamines with cardo groups in the presence of 2P-Fe_3O_4@SiO_2-$PdCl_2$ as the catalyst. Initially, the carbonylation and condensation reaction of 4,4′-di(3-iodophenoxy)diphenyl sulfone **1a**, carbon monoxide, and 9,9-bis[4-(4-aminophenoxy)phenyl]fluorene **2a** were

studied to screen the optimal reaction conditions including solvents, bases, reaction temperatures, and palladium quantities; the results are given in Table 1. At first, various organic bases including 1,4-diazabicyclo[2,2,2]octane (DABCO), *n*-Bu_3N, 4-(dimethylamino)pyridine (DMAP) and 1,8-diazabicyclo[5,4,0]-7-undecene (DBU) were tested at 120 °C in DMAc. The use of DBU as base was found to be the most efficient and furnished the polymer **3aa** with high inherent viscosity of 0.77 dL/g (entries 1–5). Compared to the other tertiary amines used, DBU swells the polyamide apart from acting as an acid acceptor, thereby enhancing the propagation reaction [22]. Replacement of DMAc as solvent with NMP, HMPA, DMF, DMSO, or DMI did not enhance the inherent viscosity of the polymer **3aa** (entries 6–10). Lowering reaction temperature to 100 or 110 ºC generated the polymer **3aa** with lower inherent viscosities because of lower reaction rates (entries 11 and 12). The reaction rate should increase with the rise in reaction temperature; however, the solubility of carbon monoxide in DMAc decreased gradually with increasing the reaction temperature. The reaction run at 130 or 140 °C also produced the polymer **3aa** with a comparatively low inherent viscosity since the actual rate of the reaction

Table 1 Screening of polymerization reaction conditions

Entry	Base	Pd loading (mol%)	PPh_3 (mol%)	Solvent	Temp. (°C)	Time (h)	η_{inh}[a] (dL/g)
1	DABCO	6	0	DMAc	120	20	0.41
2	*n*-Bu_3N	6	0	DMAc	120	24	0.27
3	DMAP	6	0	DMAc	120	24	0.19
4	DBU	6	0	DMAc	120	12	0.77
5	DBU	6	0	DMAc	120	24	0.76
6	DBU	6	0	NMP	120	20	0.49
7	DBU	6	0	HMPA	120	20	0.54
8	DBU	6	0	DMF	120	14	0.65
9	DBU	6	0	DMSO	120	14	0.61
10	DBU	6	0	DMI	120	24	0.37
11	DBU	6	0	DMAc	110	18	0.63
12	DBU	6	0	DMAc	100	24	0.46
13	DBU	6	0	DMAc	130	15	0.65
14	DBU	6	0	DMAc	140	15	0.54
15	DBU	3	0	DMAc	120	12	0.38
16	DBU	3	0	DMAc	120	24	0.56
17	DBU	10	0	DMAc	120	8	0.78
18[b]	DBU	6	24	DMAc	120	16	0.36
19[b]	DBU	6	96	DMAc	120	12	0.79

Reaction conditions: **1a** (0.5 mmol), **2a** (0.51 mmol), base (1.2 mmol), solvent (2.5 mL), and 2P-Fe_3O_4@SiO_2-$PdCl_2$ (0.03 mmol) under 1 atm of CO

[a]Measured with a concentration of 0.5 g/dL in DMAc at 30 °C

[b]$PdCl_2(PPh_3)_2$ (0.03 mmol) was used

was lower than that of the reaction performed at 120 °C (entries 13 and 14). We next studied the influence of the palladium catalyst quantity on the model reaction and found that the use of 6 mol% palladium catalyst was the best choice. Reducing the catalyst quantity to 3 mol% resulted in a lower inherent viscosity of polymer **3aa** and demanded a longer reaction time (entry 16). Increasing the catalyst quantity to 10 mol% could enhance the reaction rate, but no significant increase in the inherent viscosity of the polymer was observed (entry 17). It was reported that the synthesis of aromatic polyamides via $PdCl_2(PPh_3)_2$-catalyzed carbonylative polycondensation generally requires the use of an excess of PPh_3 as ligand to prohibit the production of palladium black [22–30]. We found that employment of 6 mol% $PdCl_2(PPh_3)_2$ and 24 mol% PPh_3 as the catalytic system gave a low inherent viscosity of the polymer and the generation of palladium black was observed clearly (entry 18). However, when 6 mol% $PdCl_2(PPh_3)_2$ and 96 mol% PPh_3 were used, the polymer **3aa** with higher molecular weight could also be generated (entry 19). Thus, the optimal polymerization reaction conditions were the use of 6 mol% 2P-Fe_3O_4@SiO_2-$PdCl_2$ with DBU as base at 120 °C in DMAc as solvent under 1 atm of CO for 12 h without addition of PPh_3 (Table 1, entry 4).

Having established the optimized polycondensation reaction conditions, we next investigated the heterogeneous carbonylation and condensation reaction of aromatic diiodides bearing ether sulfone linkages **1a–b**, carbon monoxide, and aromatic diamines with cardo groups **2a–d** as presented in Scheme 3, and the results are provided in Table 2. The novel aromatic polyamides containing both sulfone linkages and cardo groups **3aa–3bd** were prepared in high yields of 92–95% with higher inherent viscosities between 0.70 and 0.77 dL/g and could be readily converted into

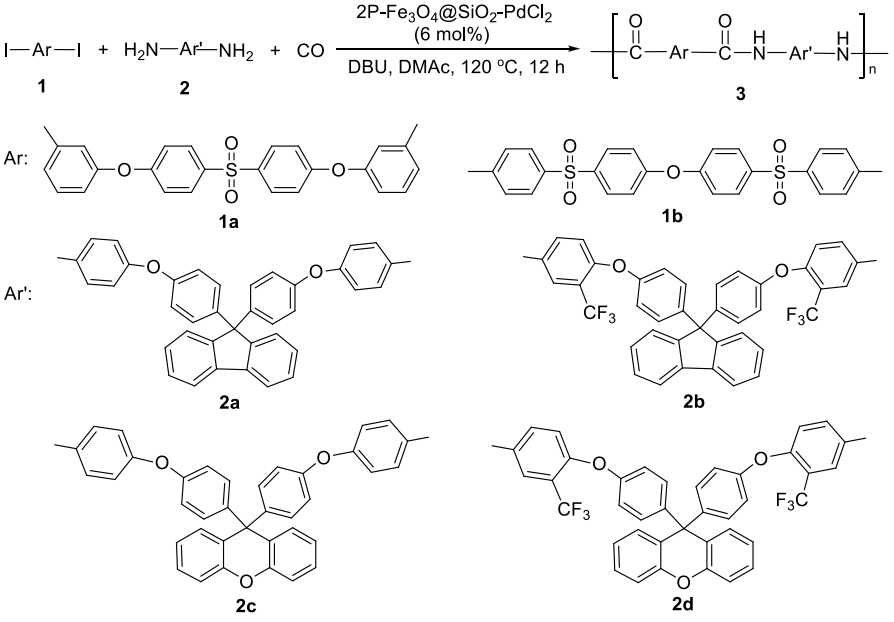

Scheme 3 Synthesis of the polymers **3aa–3bd**

Table 2 Physical properties and elemental analysis of the polymers

Polymer	Diiodide/diamine	Yield (%)	η_{inh}[a] (dL/g)	Formula	Elemental analysis			
						C (%)	H (%)	N (%)
3aa	**1a/2a**	95	0.77	$(C_{63}H_{42}N_2O_8S)_n$	Calcd	76.66	4.29	2.84
					Found	75.89	4.36	2.51
3ab	**1a/2b**	93	0.71	$(C_{65}H_{40}F_6N_2O_8S)_n$	Calcd	69.51	3.59	2.49
					Found	68.95	3.37	2.23
3ac	**1a/2c**	92	0.70	$(C_{63}H_{42}N_2O_9S)_n$	Calcd	75.44	4.22	2.79
					Found	74.63	4.18	2.51
3ad	**1a/2d**	94	0.73	$(C_{65}H_{40}F_6N_2O_9S)_n$	Calcd	68.54	3.54	2.46
					Found	68.13	3.28	2.29
3ba	**1b/2a**	93	0.72	$(C_{63}H_{42}N_2O_9S_2)_n$	Calcd	73.10	4.09	2.71
					Found	72.42	4.16	2.38
3bb	**1b/2b**	94	0.74	$(C_{65}H_{40}F_6N_2O_9S_2)_n$	Calcd	66.66	3.44	2.39
					Found	66.21	3.15	2.42
3bc	**1b/2c**	95	0.70	$(C_{63}H_{42}N_2O_{10}S_2)_n$	Calcd	71.99	4.03	2.67
					Found	71.25	3.94	2.39
3bd	**1b/2d**	94	0.73	$(C_{65}H_{40}F_6N_2O_{10}S_2)_n$	Calcd	65.76	3.40	2.36
					Found	65.38	3.09	2.11

Polymerization conditions: **1** (0.5 mmol), **2** (0.51 mmol), DBU (1.2 mmol), DMAc (2.5 mL), and 2P-Fe_3O_4@SiO_2-$PdCl_2$ (0.03 mmol) at 120 °C under 1 atm of CO for 12 h

[a]Inherent viscosity determined at a concentration of 0.5 g/dL in DMAc at 30 °C

flexible, transparent, and tough polyamide films via casting from their solutions in DMAc, revealing that the polyamides with comparatively higher molecular weights could be easily synthesized via the heterogeneous palladium-catalyzed carbonylation and condensation reaction. The molecular weight of polymer **3aa** having inherent viscosity of 0.77 dL/g was determined by GPC in DMF relative to narrow polystyrene standards. The GPC trace was unimodal with polydispersity of 1.8. The chromatogram demonstrated that the relative M_n and M_w values were 85,000 and 154,000, respectively. The elemental analysis results of these polyamides are also provided in Table 2. In general, the carbon values determined were slightly lower than the calculated ones for the proposed polymer structures because of moisture intake, and the elemental analysis values are close to the calculated ones. The chain structures of the polymers **3aa–3bd** were identified by applying FTIR and ^{1}H NMR spectroscopy. The FTIR spectra of all the polyamides display characteristic absorption peaks at 3320–3450 cm^{-1} (N–H stretching) and 1650–1670 cm^{-1} (C=O stretching) based on amide linkages, at 1220–1235 cm^{-1} (C–O–C stretching) corresponding to aryl ether linkages, as well as 1318 and 1153 cm^{-1} (-SO_2- stretching) due to sulfone linkages, which supporting their chain structures. Besides, the FTIR spectra of polymers **3ab**, **3ad**, **3bb**, and **3bd** show an absorption peak at 1135–1145 cm^{-1} (C–F stretching) owing to CF_3 groups. The FT-IR spectra of the polymers **3aa–3bd** are presented in Fig. 2. In the ^{1}H-NMR spectra of polymers **3aa–3bd**, the proton resonance signals of amide linkages appear as a sharp singlet at $\delta = 10$–11 ppm, and

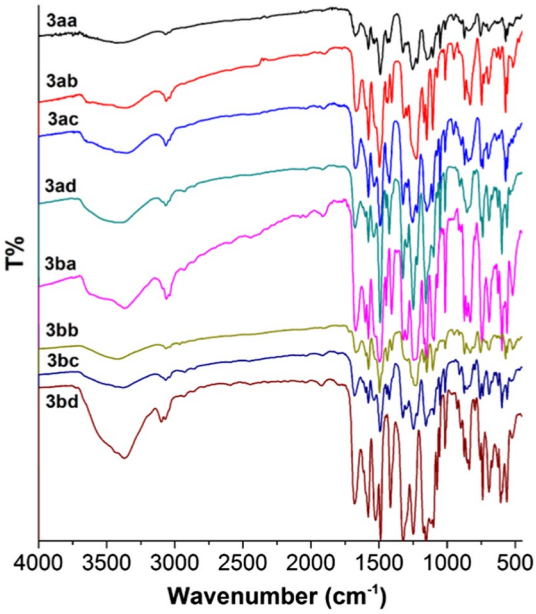

Fig. 2 FT-IR spectra of the polymers **3aa**–**3bd**

other aromatic proton peaks could also be assigned in the polymer structures proposed. Figure 3 presents a typical ^{1}H-NMR spectrum of the polymer **3ab**. The above results indicate that the polyamides containing both sulfone linkages and cardo groups **3aa–3bd** have the expected chemical structures.

Polymer solubility and crystallinity

The solubility behavior of the polyamides containing both sulfone linkages and cardo groups **3aa–3bd** was evaluated by dissolving 10 mg of the powdery samples in 1 mL of various organic solvents at room temperature, and the results are listed in Table 3. As presented in Table 3, polymers **3aa–3bd** could easily be dissolved in polar aprotic organic solvents including DMAc, NMP, DMF, DMSO and even dissolved in less polar pyridine and tetrahydrofuran at room temperature within 3 h. In addition, the polyamides **3bc** and **3bd** derived from aromatic diiodide **1b** and aromatic diamines **2c–d** exhibited better solubility than other polymers and could be swelled in acetone at room temperature due to the existence of relatively higher contents of sulfone and ether linkages in the polymer backbone. However, all these polyamides could not be dissolved or swelled in chloroform, toluene, or ethanol even on heating. The excellent solubility of polyamides **3aa–3bd** should be attributed to the combined effects of flexible ether and sulfone linkages and bulky cardo structures in the polymer main chain, which increased the distance between polymer chains and the free volume, thereby resulting in an enhanced solubility.

The crystallinity of the polyamides containing both sulfone linkages and cardo groups was evaluated by using wide-angle X-ray diffraction (WAXD). The

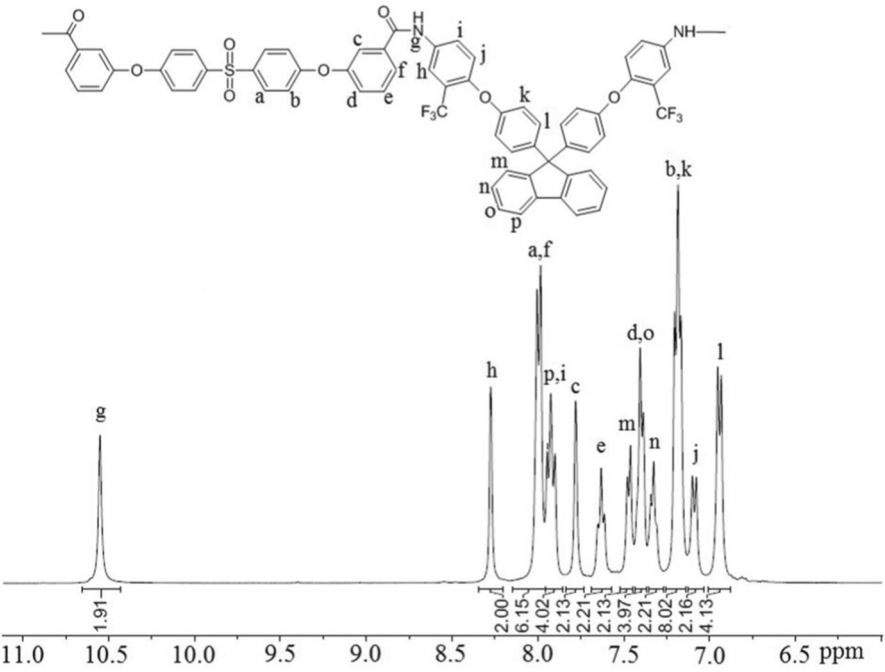

Fig. 3 ^{1}H-NMR spectrum of the polymer **3ab** (DMSO-d_6)

Table 3 Solubility of the polyamides containing both sulfone linkages and cardo groups **3aa–3bd**

Solvent	**3aa**	**3ab**	**3ac**	**3ad**	**3ba**	**3bb**	**3bc**	**3bd**
NMP	++	++	++	++	++	++	++	++
DMAc	++	++	++	++	++	++	++	++
DMF	++	++	++	++	++	++	++	++
DMSO	++	++	++	++	++	++	++	++
Pyridine	++	++	++	++	++	++	++	++
THF	++	++	++	++	++	++	++	++
Acetone	–	–	–	–	–	–	+–	+–
Chloroform	–	–	–	–	–	–	–	–
Toluene	–	–	–	–	–	–	–	–
Ethanol	–	–	–	–	–	–	–	–

++Soluble at room temperature in 3 h

+Soluble at room temperature in 24 h

+–Partially soluble or swelling at room temperature

–Insoluble

diffraction patterns illustrated in Fig. 4 indicate that the polymers **3aa–3bd** are completely amorphous, which could be attributed to the incorporation of flexible ether and sulfone linkages and bulky cardo structures into polymer backbone, which led to poor packing of polymer chains. The outstanding solubility

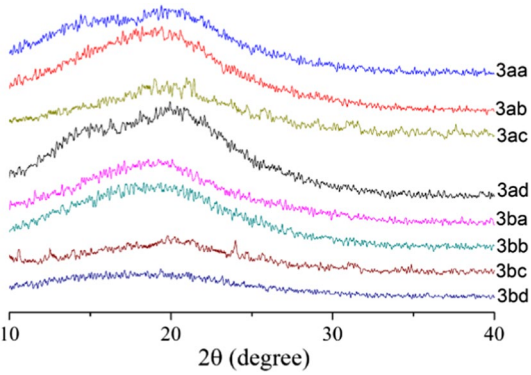

Fig. 4 WAXD patterns of the polymers **3aa–3bd**

of the polymers **3aa–3bd** in organic solvents should arise from their amorphous structures.

Thermal properties

The thermal behavior of the polyamides containing both sulfone linkages and cardo groups was investigated with DSC and TGA, and the results are provided in Table 4. Figure 5 presents DSC traces of polymers **3aa–3bd**. It was evident that there were no melting endothermic peaks on their DSC traces, which revealing very little crystalline structures. The results of DSC analysis were in accordance with the WAXD measurements of the polymers **3aa–3bd**. The polymers **3aa–3bd** had higher glass transition temperatures (T_g) between 241 and 283 °C owing to the presence of strong polar sulfone linkages and rigid cardo groups in the polymer chain. In general, the polymers **3aa–3ad** derived from aromatic diiodide **1a** exhibited relatively lower T_g values of 241–254 °C due to the existence of higher content of flexible ether linkages, while polymers **3ba–3bd** derived

Table 4 Thermal properties of the polyamides **3aa–3bd**

Polymer	T_g (°C)	T_5[a] (°C)	T_{10}[b] (°C)	R_w[c] (%)
3aa	242	448	477	63
3ab	245	453	491	58
3ac	254	438	494	54
3ad	241	475	505	47
3ba	283	444	494	56
3bb	280	471	498	59
3bc	265	440	486	52
3bd	256	447	480	55

[a] T_5 the decomposition temperature at 5% weight loss

[b] T_{10} the decomposition temperature at 10% weight loss

[c] R_w residual weight retention at 800 °C in nitrogen

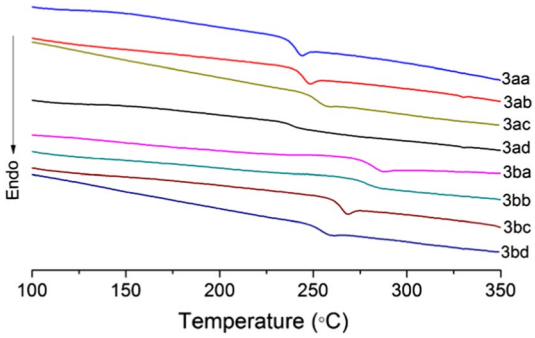

Fig. 5 DSC curves of the polymers **3aa–3bd**

from aromatic diiodide **1b** displayed relatively higher T_g values of 256–283 °C owing to the presence of higher content of strong polar sulfone linkages. In addition, polymers **3ba** and **3bb** displayed high T_g values of 280–283 °C, which may be attributed to the combined effects of higher content of strong polar sulfone linkages and more rigid fluorene cardo groups in the polymer backbone, which resulted in an increase in the interaction of polymer chains.

As seen from Table 4, the design of aromatic polyamides with the incorporation of both polar sulfone linkages and bulky cardo groups imparts not only outstanding solubility but also high thermal stability. From TGA traces of the polymers **3aa–3bd** shown in Fig. 6, we found that these polyamides did not exhibit significant weight losses before 425 ºC in nitrogen. However, when the temperature was over 450 °C, a rapid thermal decomposition reaction occurred. Polymers **3aa–3bd** had the temperatures at 5 and 10% weight loss in the range of 438–475 and 477–505 °C, respectively, in nitrogen. In addition, the polyamides **3aa–3bd** remained 47–63% of original weight at 800 °C in nitrogen.

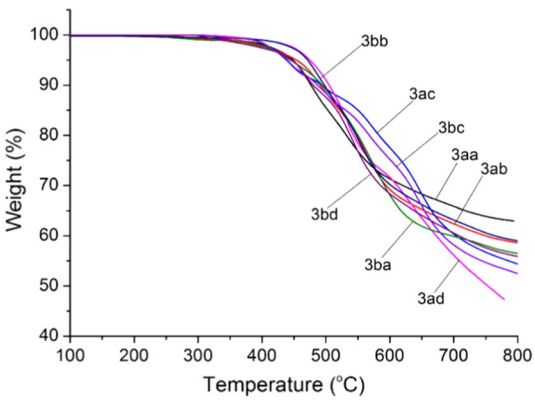

Fig. 6 TGA curves of the polymers **3aa–3bd**

Mechanical properties

Polyamides **3aa–3bd** could be easily converted into transparent, strong, and flexible polymer films via casting their DMAc solutions (15 wt% solid content) on glass plates, followed by evaporating DMAc and drying at 110 °C for 2 h, at 170 °C for 1 h, and at 190 °C in vacuo for 2 h. The unoriented cardo poly(ether sulfone amide) films were then utilized to measure the mechanical properties, and the results are given in Table 5. The tensile strengths, tensile moduli, and elongations at breakage of these polyamide films were found to be in the range of 78.8–84.4 MPa, 2.08–2.57 GPa and 10.2–12.5%, respectively. Polymer **3ad** derived from **1a** and **2d** exhibited the lowest tensile strength and tensile modulus due to the presence of higher content of flexible ether linkages and bulky CF_3 groups, which resulted in a decrease in the interaction of polymer chains. In contrast, polymer **3ba** based on **1b** and **2a** showed the highest tensile strength and tensile modulus owing to the existence of higher content of strong polar sulfone linkages and more rigid fluorene cardo groups, which led to an increase in the interaction of polymer chains.

Optical properties

The optical transparency of these polymer films with thickness of 20–25 μm was evaluated by using UV–vis spectroscopy, and their UV–vis spectra are illustrated in Fig. 7. The transmittances of the polymer films were measured at the wavelengths ranging from 300 to 800 nm, and their transmittances at several wavelengths are provided in Table 6. As seen from Table 6, the cut-off wavelengths of these new polyamide films were ranged from 338 to 368 nm and the 80% transmission wavelengths were in the range of 439–536 nm. In comparison, the polyamide films derived from aromatic diiodide **1a** showed slightly shorter cut-off wavelengths than the corresponding ones derived from aromatic diiodide **1b** due to the presence of relatively higher content of flexible ether linkages in the polymers **3aa–3ad**, which led to a decrease in the interaction of polymer chains. Polymer **3ad** showed the best transparency with cut-off wavelength at 338 nm and transmittance of 80% at 439 nm owing to the combined effects of high content of ether linkages and fluorinated substituents in the polymer backbone. This can be explained by the decrease

Table 5 Mechanical properties of the polyamides **3aa–3bd**

Polymer	Tensile strength (MPa)	Tensile modulus (GPa)	Elongation at break (%)
3aa	81.9	2.25	11.7
3ab	81.1	2.17	12.0
3ac	80.6	2.20	12.3
3ad	78.8	2.08	12.5
3ba	84.4	2.57	10.2
3bb	82.2	2.32	11.4
3bc	82.7	2.36	11.2
3bd	81.3	2.24	11.8

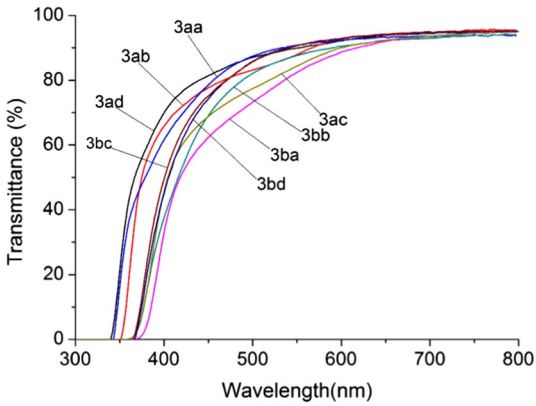

Fig. 7 UV–vis spectra of the polyamide films

Table 6 Optical properties of the polyamides **3aa–3bd**

Sample	λ_{cut} [a] (nm)	Transmittance (%)			$\lambda_{80\%\ trans}$ [b] (nm)	Refractive indices		
		400 (nm)	500 (nm)	600 (nm)		n_{TE} [c]	n_{TM} [d]	n_{AV} [e]
3aa	342	62	88	92	456	1.6874	1.6815	1.6854
3ab	351	66	83	92	466	1.6835	1.6757	1.6809
3ac	359	45	77	90	518	1.6813	1.6749	1.6792
3ad	338	70	87	93	439	1.6995	1.6938	1.6976
3ba	368	33	73	89	536	1.6754	1.6682	1.6730
3bb	359	38	82	91	489	1.6778	1.6705	1.6754
3bc	365	50	86	93	471	1.6806	1.6745	1.6786
3bd	366	45	85	92	470	1.6783	1.6715	1.6760

[a] λ_{cut} cutoff wavelength

[b] $\lambda_{80\%\ trans}$ 80% transmission wavelength

[c] n_{TE} the in-plane refractive index at 632.8 nm at ambient temperature

[d] n_{TM} the out-of-plane refractive index at 632.8 nm at ambient temperature

[e] Average refractive index

$n_{AV} = [(2n_{TE}^2 + n_{TM}^2)/3]^{1/2}$

in the intermolecular interaction caused by the presence of high content of flexible ether linkages and bulky CF_3 groups. The optical transmittance of these polyamides is generally below 80% at 450 nm, which is lower than that of the polyimides containing spirobifluorene structure in the side chain [46]. As shown in Table 6, the in-plane (n_{TE}) and out-of-plane (n_{TM}) refractive indices of the polymer films determined at 632.8 nm ranged from 1.6754 to 1.6995 and 1.6682 to 1.6938, respectively. All the polymer films exhibited higher n_{TE} values than n_{TM}, revealing that the macromolecular chains were preferentially aligned in the film plane. The average refractive index values (n_{AV}) of these polymers ranged between 1.6730 and 1.6976. Polymer **3ad** displayed the highest n_{AV} value among the prepared polymers due to the

presence of both high content of flexible ether linkages and bulky CF_3 groups in the polymer chain.

Palladium leaching and recycle of the catalyst

Recyclability and palladium leaching of this immobilized palladium catalyst were evaluated in the carbonylation and condensation reaction of aromatic diiodide **1a**, carbon monoxide, and aromatic diamine **2a** for the synthesis of polymer **3aa** under the optimal polycondensation reaction conditions. After completion of the carbonylative polymerization reaction, the reaction solution was further diluted with DMAc and the immobilized palladium catalyst could be conveniently separated from polymer **3aa** by simply placing a magnet near the reaction tube. The content of residual palladium in polymer **3aa** was measured to be 5.8 ppm by ICP-AES analysis. Thus, the leaching of palladium species into the desired polymer was not absolutely ruled out, but appeared to be negligible. After being washed with DMAc (2 mL), deionized water (2 mL), acetone (2 mL), and dried at 100 °C in vacuo for 2 h, the recovered catalyst was directly utilized in the next polymerization cycle. The recovered palladium catalyst was then employed for seven consecutive polymerization cycles with fresh monomers under the identical polymerization conditions, and the results are provided in Table 7. As seen from Table 7, almost consistent η_{inh} value and the yield of polymer **3aa** were observed in eight consecutive polymerization cycles, which implying that 2P-Fe_3O_4@SiO_2-$PdCl_2$ could be reused at least 7 times without any apparent loss of catalytic efficiency. The recycle rate of the catalyst was over 98% for the eight consecutive polymerization cycles. As seen from the TEM images of the recovered palladium catalyst (Fig. 8b) and the fresh one (Fig. 8a), no obvious differences in the morphology and dispersion of particles were observed, indicating that no palladium black was formed during the process of polycondensation. The excellent reusability and negligible Pd leaching of 2P-Fe_3O_4@SiO_2-$PdCl_2$ might be mainly due to the stronger chelating action between palladium atom and the bidentate phosphine ligand.

Table 7 Recycling of the 2P-Fe_3O_4@SiO_2-$PdCl_2$ catalyst

Entry	Pd catalyst	Yield (%)	η_{inh}[a] (dL/g)	Recycle rate of Pd (%)	Entry	Pd catalyst	Yield (%)	η_{inh}[a] (dL/g)	Recycle rate of Pd (%)
1	Fresh	95	0.77	99	5	Recycle 4	93	0.75	98
2	Recycle 1	95	0.76	99	6	Recycle 5	94	0.74	99
3	Recycle 2	94	0.77	98	7	Recycle 6	95	0.75	99
4	Recycle 3	95	0.75	99	8	Recycle 7	94	0.74	98

Polymerization conditions: **1a** (0.5 mmol), **2a** (0.51 mmol), DBU (1.2 mmol), DMAc (2.5 mL), and 2P-Fe_3O_4@SiO_2-$PdCl_2$ (0.03 mmol) at 120 °C under 1 atm of CO for 12 h

[a]Inherent viscosity determined at a concentration of 0.5 g/dL in DMAc at 30 °C

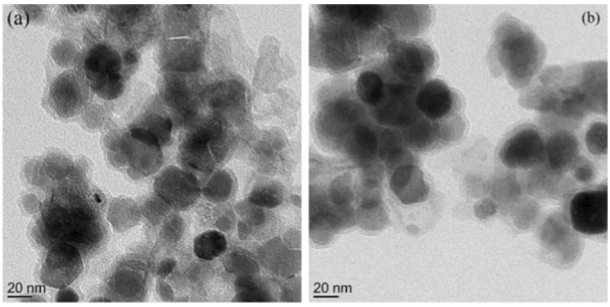

Fig. 8 TEM images of the fresh 2P-Fe_3O_4@SiO_2-$PdCl_2$ (**a**) and recycled 2P-Fe_3O_4@SiO_2-$PdCl_2$ after eighth run (**b**)

Conclusion

A new, efficient and practical synthetic route to aromatic polyamides containing both sulfone linkages and cardo groups with higher molecular weights has been developed through heterogeneous palladium-catalyzed carbonylation and condensation reaction of aromatic diiodides bearing ether sulfone linkages, carbon monoxide, and aromatic diamines with cardo groups by using a bidentate phosphine ligand-modified magnetic nanoparticles-anchored palladium complex [2P-Fe_3O_4@SiO_2-$PdCl_2$] as the catalyst. The resulting cardo poly(ether sulfone amide)s displayed outstanding solubility and high thermal stability with the glass transition temperatures between 241 and 283 °C, the temperatures at 5% weight loss ranging from 438 to 475 °C in nitrogen. These polymer films exhibited good mechanical properties with tensile strengths of 78.8–84.4 MPa, tensile moduli of 2.08–2.57 GPa, elongations at breakage of 10.2–12.5%, and optically high transparency with cut-off wavelengths in the range of 338–368 nm. More importantly, the 2P-Fe_3O_4@SiO_2-$PdCl_2$ catalyst can be facilely separated from the desired polymer simply by placing a magnet near the reaction tube and reused at least seven times without any apparent decrease in the catalytic activity, thus making the current methodology economically and environmentally more acceptable.

Acknowledgements We thank the National Natural Science Foundation of China (Project 21664008), Natural Science Foundation of Jiangxi Province in China (Project 20181BAB203011) and Key Laboratory of Functional Small Organic Molecule, Ministry of Education (No. KLFS-KF-201704) for financial support.

References

1. Reglero Ruiz JA, Trigo-Lopez M, Garcia FC, Garcia JM (2017) Functional aromatic polyamides. Polymers 9(12):414–414
2. Liou GS, Hsiao SH (2002) Synthesis and properties of new soluble aromatic polyamides and polyimides on the basis of *N, N′*-bis(3-aminobenzoyl)-*N, N ′*- diphenyl-1,4-phenylenediamine. J Polym Sci Part A Polym Chem 40:2564–2574

3. Liaw DJ, Hsu PN, Chen WH, Lin SL (2002) High glass transitions of new polyamides, polyimides, and poly(amide-imide)s containing a triphenylamine group: synthesis and characterization. Macromolecules 35:4669–4675
4. Wu SC, Shu CF (2003) Synthesis and properties of soluble aromatic polyamides derived from 2,2'-bis(4-carboxyphenoxy)-9,9'-spirobifluorene. J Polym Sci Part A Polym Chem 41:1160–1166
5. Garcia JM, Garcia FC, Serna F, de laPena JL (2010) High-performance aromatic polyamides. Prog Polym Sci 35:623–686
6. Bera D, Padmanabhan V, Banerjee S (2015) Highly gas permeable polyamides based on substituted triphenylamine. Macromolecules 48:4541–4554
7. Dewilde S, Hoogerstraete TV, Dehaen W, Binnemans K (2018) Synthesis of poly-*p*-phenylene terephthalamide (PPTA) in ionic liquids. ACS Sustainable Chem Eng 6:1362–1369
8. Pascual BS, Trigo-Lopez M, Ramos C, Sanz MT, Pablos JL, Garcia FC, Reglero Ruiz JA, Garcia JM (2019) Microcellular foamed aromatic polyamides (aramids). Structure, thermal and mechanical properties. Eur Polym J 110:9–13
9. Trigo-Lopez M, Garcia JM, Reglero Ruiz JA, Garcia FC, Ferrer R (2018) Aromatic polyamides. In: Mark HF (ed) Encyclopedia of polymer science and technology. Wiley, New Jersey, pp 1–51
10. Liou G-S, Hsiao S-H, Ishida M, Kakimoto M, Imai Y (2002) Synthesis and characterization of novel soluble triphenylamine-containing aromatic poly- amides based on *N, N*'-bis(4-aminophenyl)-*N,* N'-diphenyl-1,4-phenylenediamine. J Polym Sci Part A Polym Chem 40:2810–2818
11. Liou G-S, Hsiao S-H (2002) Polyterephthalamides with naphthoxy-pendent groups. J Polym Sci Part A Polym Chem 40:1781–1789
12. Hsiao S-H, Chen W-T (2003) Syntheses and properties of novel fluorinated polyamides based on a bis(ether-carboxylic acid) or a bis(ether amine) extended from bis(4-hydroxyphenyl)phenyl-2,2,2-trifluoroethane. J Polym Sci Part A Polym Chem 41:420–431
13. Liaw D-J, Liaw B-Y (1998) Synthesis and properties of new polyamides derived from 1,4-bis(4-aminophenoxy)-2,5-di-*tert*-butylbenzene and aromatic dicarboxylic acids. J Polym Sci Part A Polym Chem 36:1069–1074
14. Espeso JF, Ferrero E, de la Campa JG, Lozano AE, de Abajo J (2001) Synthesis and characterization of new soluble aromatic polyamides derived from 1,4-bis(4-carboxyphenoxy)-2,5-di-*tert*-butylbenzene. J Polym Sci Part A Polym Chem 39:475–485
15. Johnson RN, Farnham AG, Clendinning RA, Hale WF, Merriam CN (1967) Poly(aryl ethers) by nucleophilic aromatic substitution. I. Synthesis and properties. J Polym Sci Part A Polym Chem 5:2375–2398
16. Attwood TE, King T, Leslie VJ, Rose JB (1977) Poly(arylene ether sulphones) by polyetherification: 2. Polycondensations Polymer 18:359–364
17. Harris JE, Johnson RN (1985) Polysulfone. In: Mark HF, Bikales NB, Overberger CG, Menges G (eds) Encyclopedia of polymer science and engineering, vol 11, 2nd edn. Wiley, New York, p 196
18. Knight J, Wright WW (1983) Heat-resistant polymers. Plenum, New York, p 170
19. Brode GL, Kwiatkowski GT, Bedwin AW (1974) High temperature polymers. II. High temperature polymers from 4,4′-[sulfonylbis(*p*-phenyleneoxy)]dianiline. J Polym Sci Part A Polym Chem 12:575–587
20. Chiriac C, Stille JK (1977) Polyaramides containing sulfone ether units. Macromolecules 10:712–713
21. Mehdipour-Ataei S, Sarrafi Y, Hatami M, Akbarian-Feizi L (2005) Poly(sulfone ether amide amide) s as a new generation of soluble, thermally stable polymers. Eur Polym J 41:491–499
22. Yoneyama M, Kakimoto M, Imai Y (1988) Novel synthesis of aromatic poly- amides by palladium-catalyzed polycondensation of aromatic dibromides, aromatic diamines, and carbon monoxide. Macromolecules 21:1908–1911
23. Yoneyama M, Kakimoto M, Imai Y (1989) Synthesis of aliphatic-aromatic polyamides by palladium-catalyzed polycondensation of aliphatic diamines, aromatic dibromides, and carbon monoxide. J Polym Sci Part A Polym Chem 27:1985–1991
24. Turner SR, Perry RJ, Blevins RW (1992) High molecular weight aromatic polyamides from aromatic diiodides and diamines. Macromolecules 25:4819–4820
25. Perry RJ, Turner SR, Blevins RW (1993) Synthesis of linear, high molecular weight aromatic polyamides by the palladium-catalyzed carbonylation and condensation of aromatic diiodides, diamines, and carbon monoxide. Macromolecules 26:1509–1513
26. Perry RJ, Turner SR, Blevins RW (1994) Palladium-catalyzed formation of poly(imide-amides). 1. reactions with diiodo imides and diamines. Macromolecules 27:4058–4062

27. Ueda M, Yokoo T (1994) Synthesis of poly(ether-ketone-amide)s by palladium- catalyzed polycondensation of aromatic dibromides containing ether ketone structure, aromatic diamines, and carbon monoxide. J Polym Sci Part A Polym Chem 32:2065–2071
28. Ueda M, Yokoo T, Nakamura T (1994) Synthesis of poly(ether-sulfone-amide)s by palladium-Catalyzed Polycondensation of aromatic dibromides containing ether sulfone structure, aromatic diamines, and carbon monoxide. J Polym Sci Part A Polym Chem 32:2989–2995
29. Perry RJ, Turner SR, Blevins RW (1995) Palladium-catalyzed formation of poly(imide-amides). 2 reactions with chloroiodophthalimides and diamines. Macromolecules 28:2607–2610
30. Rabani G, Kraft A (2002) Synthesis of poly(ether-esteramide) elastomers by palladium-Catalyzed Polycondensation of aromatic diiodides with telechelic diamines and carbon monoxide. Macromol Rapid Commun 23:375–379
31. Stevens PD, Li G, Fan J, Yen M, Gao Y (2005) Recycling of homogeneous Pd catalysts using superparamagnetic nanoparticles as novel soluble supports for Suzuki, Heck, and Sonogashira cross-coupling reactions. Chem Commun 35:4435–4437
32. Baruwati B, Guin D, Manorama SV (2007) Pd on surface-modified $NiFe_2O_4$ nanoparticles: a magnetically recoverable catalyst for Suzuki and Heck reactions. Org Lett 9:5377–5380
33. Jin M-J, Lee D-H (2010) A practical heterogeneous catalyst for the Suzuki, Sonogashira, and Stille coupling reactions of unreactive aryl chlorides. Angew Chem Int Ed 49:1119–1122
34. Shylesh S, Wang L, Thiel WR (2010) Palladium(II)-phosphine complexes supported on magnetic nanoparticles: filtration-free, recyclable catalysts for Suzuki-Miyaura cross-coupling reactions. Adv Synth Catal 352:425–432
35. Li P, Wang L, Zhang L, Wang G-W (2012) Magnetic nanoparticles-supported palladium: a highly efficient and reusable catalyst for the Suzuki, Sonogashira, and Heck reactions. Adv Synth Catal 354:1307–1318
36. Tang H, Huang B, Zhu X, Cai M (2018) Synthesis of poly(ether ketone amide)s containing 4-aryl-2,6-diphenylpyridine moieties by a heterogeneous palladium- catalyzed polycondensation of aromatic diiodides, aromatic diamines, and carbon monoxide. Polym Adv Technol 29:2204–2215
37. Liu L, Zou F, Zhang R, Cai M (2019) Synthesis of new fluorinated aromatic poly (ether ketone amide)s containing cardo structures by a heterogeneous palladium-catalyzed carbonylative polycondensation. Polym Adv Technol 30:58–69
38. Liu L, Li J, Yan T, Cai M (2020) Novel preparation of poly(arylene ether sulfone amide)s via supported palladium-catalyzed carbonylative polymerization. Polym Bull 77:1951–1968
39. Hu Z, Li S, Zhang C (2007) Synthesis and properties of polyamide-imides containing fluorenyl cardo structure. J Appl Polym Sci 106:2494–2450
40. Yang CP, Su YY, Hsu MY (2006) Synthesis and properties of fluorinated polyamides and poly(amide imide)s based on 9,9-bis[4-(4-amino-2-trifluoro- methylphenoxy)phenyl]fluorene, aromatic dicarboxylic acids, and various monotrimellitimides and bistrimellitimides. Colloid Polym Sci 284:990–1000
41. Sheng S, Li T, Jiang J, He W, Song C (2010) Synthesis and properties of novel polyamides containing sulfone-ether linkages and xanthene cardo groups. Polym Int 59:1014–1020
42. Sheng S-R, Ma C-X, Jiang J-W, Li Q, Song C-S (2011) Optically high transparency and light color of organosoluble fluorinated polyamides with bulky xanthene pendent groups. Polym Adv Technol 22:2523–2532
43. Yang CP, Lin JH (1995) Syntheses and properties of aromatic polyamides and polyimides based on 3,3-bis[4-(4-aminophenoxy)phenyl]phthalimidine. Polymer 36:2607–2614
44. Liaw DJ, Liaw BY, Chung CY (1999) Synthesis and characterization of new cardo polyamides derived from 8,8-bis[4-(4-aminophenoxy)phenyl]tricycle- $[5.2.1.0^{2,6}]$decane. Macromol Chem Phys 200:1023–1027
45. Liaw DJ, Liaw BY, Chung CY (2000) Synthesis and characterization of new cardo polyamides and polyimides containing *tert*-butylcyclohexylidene units. Macromol Chem Phys 201:1887–1893
46. Wen P, He R, Li X-D, Lee M-H (2017) Synthesis and characterization of high refractive index and low birefringence polyimides containing spirobifluorene in the side chain. Polymer 117:76–83